I S A V

Journal of Theoretical and Applied Vibration and Acoustics

journal homepage: http://tava.isav.ir

Fluid-structure interaction and vibration analysis of the fuel system of a turbofan engine with optimal dimensions

Mohammad Reza Elhami[a*], Mohammad Javad Shirazi Parsa[b]

[a]*Associate Professor, Mechanical Engineering Faculty, Imam Hossein Comprehensive University, Tehran, Iran.*

[b]*M.Sc. Graduate, Mechanical Engineering Faculty, Imam Hossein Comprehensive University, Tehran, Iran.*

ARTICLE INFO

Article history:
Received 10 January 2020

Received in revised form
14 October 2020

Accepted 9 December 2020

Available online 25 December 2020

Keywords:
FSI,

fuel system,

pipe conveying fluid,

Vibration,

Optimization.

ABSTRACT

This paper investigates the main problem of combustion instability in turbofan engines which is usually the unbalanced fuel pump causing turbulences in the fuel flow as well as vibrations in the fuel pipes of the system.At first, the equations of frequencies are derived analytically in the direct and knee joint pipes to verify the results of the Abaqus software. The results show an acceptable accuracy of the Abaqus software to solve the problem of the fluid coupling structure. The results show that the vibration frequency of this part of the fuel transfer system (2.5 to 18 Hz in different modes) is very low compared to the entire engine operational frequency (around 140 Hz). The maximum transverse displacement (range) is relatively significant (up to 16 mm), which is noticeable with respect to the overall dimensions of the system. However, this amplitude would decrease by two clamped-ended with two fastened belts. In the following part, optimization of the system parameters was done using the Design-expert Software and NSGA II code. The basic parameters studied in this paper are radius, thickness, and length of the pipe with different spans, as well as the turbulence inflow. Optimal mode is achieved with laminar velocity contours. In conclusion, the outflow disturbance has been decreased, which consequently reduces the turbulence of the fuel that can improve combustion stability.

[*] Corresponding author:
E-mail address: melhami@ihu.ac.ir (M. R. Elhami)

http://dx.doi.org/10.22064/tava.2021.121014.115

1. Introduction

The fluid-structure interaction (FSI) phenomenon often occurred in the systems containing fluid. FSI in a system is a dual-phase problem in which fluid flow leads to vibrations in solid structures, and solid forms boundary conditions of the fluid problem. For instance, the airflow around the wing of the plane changes the shape of the tip (though partially), which will subsequently change the airflow pattern around the wings. In general, an FSI system can be considered as weakly coupled or strongly coupled. The fluid flow usually causes deformation in the body structure and thus causes turbulences in the flow field; then the condition called strongly coupled FSI happens. However, if the deformation of the solid body does not cause significant changes in the fluid field, it will be called weakly coupled FSI. These systems are known as weakly coupled systems, which are the case of this research.

In 1995, Morand and Ohayon[1] presented a number of numerical models for linear vibration modeling of internal elastic coupling structures. They have also focused on hydrostatic oscillations and structural noise in their applications. In 2001, Dowl and Hall [2] examined various fluid and structure coupling models. They also described various physical models for a time-dependent motion for fluid and then discussed the distinction between linear and nonlinear models in time or frequency range and time step harmonic equilibrium of identification systems. In this paper, the aerodynamics of an airfoil and its aerodynamic diagrams have also been studied. In 2004, Michler [3] compared the discrete and continuous solutions for numerical simulation of fluid-structure interaction. For evaluation of the accuracy of these methods, their cost and computational efficiency are also compared. In a discrete method at any time step, only a repetition of the fluid-structure interaction is required, resulting in a lower computational cost than the continuous method at any time step. In contrast to the discrete (component) method, it is a continuous method that appears to be uniquely stable and significantly more precise without any conditions. It can use a larger time step than the discrete method for the same level with higher precision. Nevertheless, computations that take place in continuous methods at any time step are more expensive than discrete methods. In 2005, Chakrabarti[4] introduced a wide range of numerical computing techniques in the field of fluid mechanics and numerical calculations for the fluid effect on marine structures. In 2012, Hou *et al.* [5], in their study of numerical methods for fluid and structure interaction, addressed a nonlinear multi-physical phenomenon. The immersion method is an irregular mesh method. In the article, they examined the basic formulation of the immersion fringe method, immersion domain method and other immersion methods. In 2016, Tashakori and Elhami [6] studied the fluid-structure interaction phenomenon of a turbine blade. They were stimulated by using the structural and fluid flow section of ANSYS software. The results show that by increasing the speed of inlet flow, the amount of blade tip deviation increases and also its impact increases on fluid pressure exerted on the rotor. In 2016, Dubyk and Orynyak [7] analyzed the impact of the transported fluid on the natural frequencies of a pipeline. It is shown that treating fluid as an added mass for the axial vibrations can lead to significant errors. Again in 2016, Moore[8] carried out a review of noise and vibration in fluid-filled pipe systems. This review concludes with a discussion of research on identifying transmission and source characteristics of pumps. In 2017, Fong *et al*.[9] studied the vibration of damped pipeline conveying fluid with the effect of fluid-structure interaction. In this study, the natural frequency of fluid-structure interaction in pipeline conveying fluid has been investigated and analytically derived by using the finite element method. Then FSI problem with certain boundary conditions has been solved by Abaqus software. In the following stage, optimization of

the pipe parameters such as radius, thickness, and length of the pipe with different spans as well as the turbulence inflow, carried out by the Design-expert Software and NSGA II code. It should be noted that the main purpose is to acquire the specific dimensions for a portion of the fuel system to reduce the vibration range and reduce the turbulence of the fluid in order to achieve better combustion stability for the turbofan engine.

2. Fluid and structure couplings

The FSI method used in this paper is a combination of CFD† and CMS‡ methods. Generally, solving problems with multiple physics is very difficult in analytical form. Therefore, such issues are often solved using numerical and experimental methods. Advanced numerical methods and popular commercial software applications in the CFD and CMS domains that make use of these methods includes two different solutions for solving FSI problems using software, a Monolithic approach solution and Partitioned approach solving, which are described in each of these strategies. In Fig.1, the breakdown of all types of FSI solutions can be seen [10].

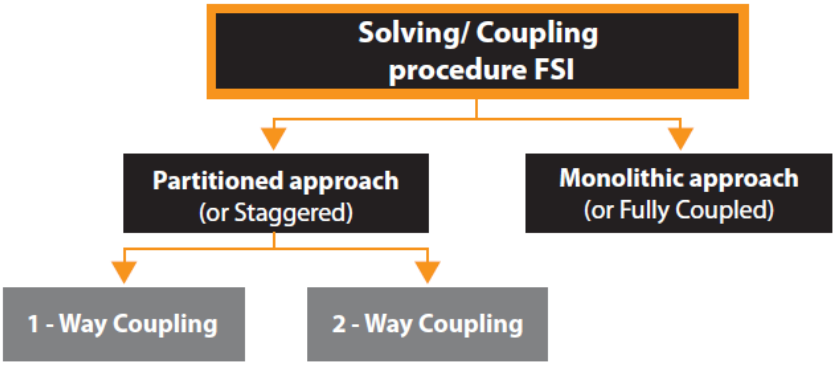

Fig. 1. Solving procedures in the FSI [10]

In this study, the partitioned approach and One-way coupling are used. In this way, each of the problems is solved individually in a separate solvent, meaning that the fluid does not change during a structural solution and vice versa. The fluid and structure equations are solved periodically in two solvents, and the information of each solution is exchanged at the point of contact of the fluid with the structure. The problem-solving process of this type is depicted in Fig. 2. The process of exchanging information at the level between the two ranges of solvers is called the solder coupler. It has two types of one-way couplings and two-way couplings.

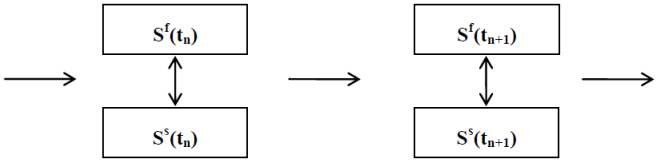

Fig. 2. Partitioned approach [11]

† - Computational Fluid Dynamics
‡ - Computational Structural Mechanics

One-way coupling is a mode that the movement of the fluid influences the structure, and the response of the structure to the fluid is neglected. As an example, in solving the issue of the ropeller of the ship, the problem is considered as a one-way coupling. Figure 3 presents a graph of the one-way coupling method.

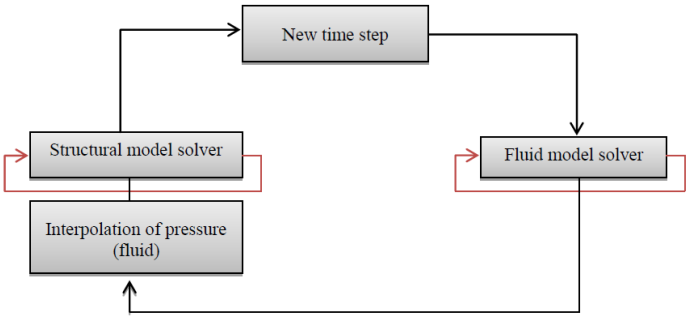

Fig.3. One-way coupling- flow chart [11]

3. Natural frequency of the straight pipe containing fluid

In this section, the natural frequency of vibrations due to fluid-structure interaction in a straight pipe containing fluid is investigated by the Galerkin method for different support conditions. Long pipes are usually modeled as Euler Bernoulli beam and they can be either clamped or simply supported on both sides. It is assumed that the fluid is non-viscous, incompressible, and deformation of the pipe is small, and gravity is neglected. Figure 4 shows the shape of a straight pipe containing flows with supports on both sides. The mathematical model of the transient vibrations of this pipe is obtained using the Hamiltonian principle:

$$\int_0^l \left[EI \frac{\partial^2 y}{\partial x^2} \frac{\partial^2}{\partial x^2}(\delta y) - m_0 v^2 \frac{\partial y}{\partial x} \frac{\partial}{\partial x}(\delta y) + m_0 \frac{\partial^2 y}{\partial x \partial t} \delta y - m_0 v \frac{\partial y}{\partial t} \frac{\partial}{\partial x}(\delta y) + (m + m_0) \frac{\partial^2 y}{\partial t^2} \delta y \right] dx = 0 \quad (1)$$

In this respect, l is the length of the straight pipe, m mass per unit length of pipe, m_0 mass of fluid per unit length of pipe, v constant flow rate, E elastic modulus of the straight pipe, I cross-sectional moment of inertia of the straight pipe, y transverse deformation of the straight pipe, x and t are the axial coordinate and time, respectively. In order to derive the integral equation (1), it is necessaryto consider the boundary conditions of the following straight pipe.

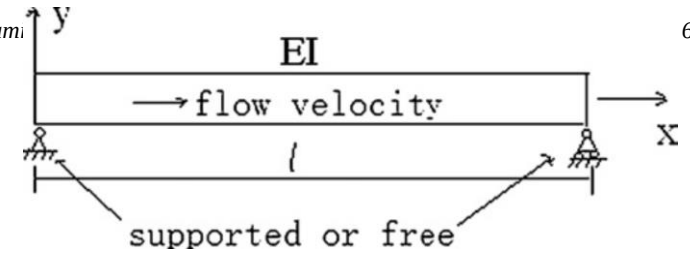

Fig. 4 Straight pipe boundary conditions containing fluid flow [12]

As for each condition, equation(1) can be simplified by the variation principle. After integration of equation (1), it can be expressed for the straight pipe vibrations containing fluid flow as follows:

$$EI\frac{\partial^4 y}{\partial x^4} + m_0 v^2 \frac{\partial^2 y}{\partial x^2} + 2m_0 v \frac{\partial^2 y}{\partial x \partial t} + (m + m_0)\frac{\partial^2 y}{\partial t^2} = 0 \quad (2)$$

Given the relative motion of the fluid, there is the Coriolis force, which is:

$$F_c = 2m_0 v \frac{\partial^2 y}{\partial x \partial t} \quad (3)$$

Equation (3) is a high-order partial derivative equation that is difficult to solve analytically, and thus, the Galerkin method can be used to approximate this equation. To separate the variables in the equation, the following should be considered.

$$y(x,t) = u(x)e^{i\omega t} \quad (4)$$

This equation is the general form of the free vibration response.

For the S-S, C-C and C-S support conditions are all δ (0) = δ (l) = 0, and for C-C state, its boundary conditions as follows:

$$u(0) = u(l) = 0 \quad , \quad u'(0) = u'(l) = 0 \quad (5)$$

Substituting into equation (3) and removing the term e iωt, the equation is obtained.

$$EI\frac{d^4 u(x)}{dx^4} + m_0 v^2 \frac{d^2 u(x)}{dx^2} + 2m_0 v \frac{du(x)}{dx}\, i\omega - (m + m_0)\omega^2 u(x) = 0 \quad (6)$$

Equation (6) is a univariable and high-order equation in which the Galerkin method can be used. If we consider the first frequency of vibrations at different boundary conditions, the natural frequency of the first four modes are obtained as follows[12]:

I. For the C-C condition:

$$\omega_i = (\beta_i)^2 \sqrt{\frac{EI}{m + m_0}} . \sqrt{1 - \frac{0.55 m_0 v^2}{EI{\beta_1}^2}} \quad i = 1,2,3,4,\ldots \quad (7)$$

$$with\ \beta_1 l = 4.730041,\ \beta_2 l = 7.853205, \beta_3 l = 10.995608, \beta_4 l = 14.137165$$

II. For the C-S condition

$$\omega_i = (\beta_i)^2 \sqrt{\frac{EI}{m+m_0}} . \sqrt{1 - \frac{0.747 m_0 v^2}{EI{\beta_1}^2}}\ , \qquad i = 1,2,3,4,\ldots \tag{8}$$

$$with\ \beta_1 l = 3.926602,\ \beta_2 l = 7.0685583, \beta_3 l = 10.210176, \beta_4 l = 13.351768$$

III. For the S-F condition

$$\omega_j = \left(\beta_j\right)^2 \sqrt{\frac{EI}{m+m_0}} . \sqrt{1 - \frac{(0.26 m_0/(m+m_0) + 0.7465) m_0 v^2}{EI{\beta_1}^2}} + 0.51\ \frac{m_0 v \beta_1}{m+m_0} i\ , \tag{9}$$

$$j = 1,2,3,4,\ldots$$

$$with\ \beta_1 l = 3.926602, \beta_2 l = 7.0685583, \beta_3 l = 10.210176, \beta_4 l = 13.351768$$

IV. For the S-S condition:

$$\omega_i = (\beta_i)^2 \sqrt{\frac{EI}{m+m_0}} . \sqrt{1 - \frac{m_0 v^2}{EI{\beta_1}^2}}\ , \quad i = 1,2,3,4,\ldots \tag{10}$$

$$with\ \beta_1 l = \pi, \beta_2 l = 2\pi, \beta_3 l = 3\pi, \beta_4 l = 4\pi$$

V. For the C-F condition:

$$\omega_j = \left(\beta_j\right)^2 \sqrt{\frac{EI}{m+m_0}} . \sqrt{1 - \frac{(1.1376 m_0/(m+m_0) + 0.2441) m_0 v^2}{EI{\beta_1}^2}} + 1.067\ \frac{m_0 v \beta_1}{m+m_0} i\ , \tag{11}$$

$$j = 1,2,3,4,\ldots$$

$$with\ \beta_1 l = 1.875104,\ \beta_2 l = 4.694091, \beta_3 l = 7.854757,\ \beta_4 l = 10.995541$$

4. Natural frequency of the curved pipe containing fluid

Consider a uniform curved pipe as in Figure 5. The curved radius R is mass per unit length *m*, modulus of elasticity *E*, the moment of inertia *I*, fluid mass per unit length *M*, and constant velocity *V*. The cross-sectional area of the flow stream is *A*, and the pressure is *P*. In this section, we review vibration analysis on the plate of this fluid-structure coupling system.

The cylindrical coordinate system is suitable for defining the knee, denoted by r,θ in the plane, and axis z, normal to the plane. The displacement is denoted by *u*, *v*, and *w*, respectively, which are positive in the positive direction of the coordinate system. Consider the *mm* element before the deformation that is transformed after the deformation, and the radius of curvature after the deformation is transformed as defined below [13].

$$\frac{1}{R'} = \frac{1}{R}\left(1 + \frac{u}{R} + \frac{1}{R}\frac{\partial^2 u}{\partial \theta^2}\right) \tag{12}$$

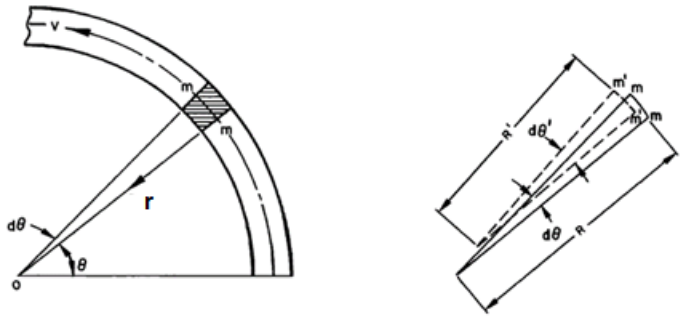

Fig. 5 the coordinates of an element [13]

It is considered that there is no deformation in the centerline of the pipe.

The differential equations for rotational motion and for translational motion in radial and tangential directions of the pipe element in Fig. 6(a), as follows:

$$\frac{\partial \bar{M}}{\partial \theta} + RF = 0 \tag{13}$$

$$\frac{\partial F}{\partial \theta} + T - RQ = mR\partial^2 u/\partial t^2 \tag{14}$$

$$\frac{\partial T}{\partial \theta} + RSq - F = mR\partial^2 w/\partial t^2 \tag{15}$$

$\bar{M}$ and T, F are the bending moment, normal force, and internal shear force, respectively; also in these relations, q is the shear stress on the inner surface, S, of the pipe, Q is the transverse force entered at the inner surface of the pipe in contact with the fluid. Consider similarly the fluid element in Fig. 6(b), acceleration of this component in tangential and radial directions, respectively:

$$a_t = \frac{\partial^2 w}{\partial t^2} - \left(\frac{V^2}{R^2}\right)\left(\frac{\partial^2 w}{\partial \theta^2} + w\right) \tag{16}$$

$$a_r = \frac{V^2}{R}\left(1 + \frac{u}{R}\right) + \left(\frac{\partial}{\partial t} + \frac{V}{R}\frac{\partial}{\partial \theta}\right)^2 u + \frac{2V}{R}\frac{\partial w}{\partial t} \tag{17}$$

Therefore, the force balance in the tangential and radial directions are as follows:

$$Q - \frac{PA}{R'} = \frac{MV^2}{R}\left(1 + \frac{u}{R}\right) + M\left(\frac{\partial^2 u}{\partial t^2} + \frac{2V}{R}\frac{\partial^2 u}{\partial t \partial \theta} + \frac{2V}{R}\frac{\partial w}{\partial t} + \frac{V^2}{R^2}\frac{\partial^2 u}{\partial \theta^2}\right) \tag{18}$$

$$A\left(\frac{\partial P}{\partial \theta}\right) + RSq = -MR\left[\frac{\partial^2 w}{\partial t^2} - \frac{V^2}{R^2}\left(\frac{\partial^2 w}{\partial \theta^2} + w\right)\right] \tag{19}$$

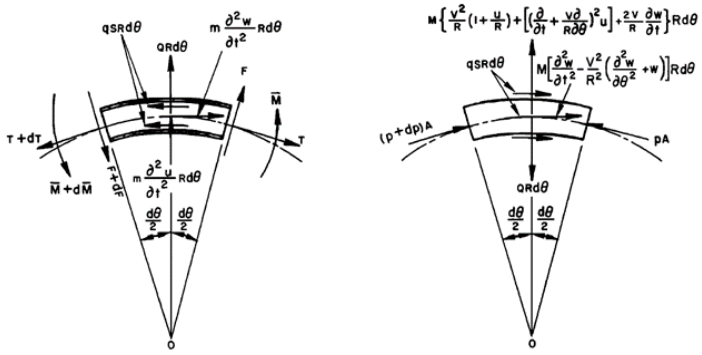

(a) **(b)**

Fig. 6 Force and Moment Enter into (a) Pipe element, (b) Fluid element [13]

The bending moment can be expressed in terms of the displacement components as

$$\bar{M} = \frac{EI}{KR}\left(\frac{\partial^2 u}{\partial \theta^2} + \frac{\partial w}{\partial \theta}\right) \tag{20}$$

$E_1I_1 = EI / k$, E_1I_1, and k are the flexible factor and the effective stiffness of the curved pipe, respectively. Considering the above equations and ignoring the higher-order terms, the partial differential equations is simplified by w of sixth order as follows:

$$\begin{aligned}\frac{\partial^6 w}{\partial \theta^6} + \left(2 + \frac{AR^2P}{E_1I_1} + \frac{MR^2V^2}{E_1I_1}\right)\frac{\partial^4 w}{\partial \theta^4} + \left(1 + \frac{AR^2P}{E_1I_1} + \frac{2MR^2V^2}{E_1I_1}\right)\frac{\partial^2 w}{\partial \theta^2} + \frac{MR^2V^2}{E_1I_1}w \\ + \frac{2MR^3V}{E_1I_1}\frac{\partial^4 w}{\partial t \partial \theta^3} + \frac{2MR^3V}{E_1I_1}\frac{\partial^2 w}{\partial t \partial \theta} + \frac{(M+m)R^4}{E_1I_1}\frac{\partial^4 w}{\partial t^2 \partial \theta^2} \\ - \frac{(M+m)R^4}{E_1I_1}\frac{\partial^2 w}{\partial t^2} = 0\end{aligned} \tag{21}$$

In which, if the flow constant velocity and pressure are set to zero, the equation is simplified as follows:

$$\frac{\partial^6 w}{\partial \theta^6} + 2\frac{\partial^4 w}{\partial \theta^4} + \frac{\partial^2 w}{\partial \theta^2} + \frac{(M+m)R^4}{E_1I_1}\left(\frac{\partial^4 w}{\partial t^2 \partial \theta^2} - \frac{\partial^2 w}{\partial t^2}\right) = 0 \tag{22}$$

It can be seen that actually, this equation is the equation of motion of free vibration of a circular ring. On the other hand, if R is tended to infinity, the equation (21) is simplified as follows:

$$EI\frac{\partial^4 w}{\partial x^4}+(AP+MV^2)\frac{\partial^2 w}{\partial x^2}+2MV\frac{\partial^2 w}{\partial t\partial x}=0 \tag{23}$$

It is observed that this equation is also the equation of motion of straight pipe as Eq. (3), with setting the pressure fluid P to zero.

Consider the following dimensionless parameters:

$$\eta = u/R \qquad \beta = M/(M+m)$$
$$\xi = w/R \qquad \tau = \left(\frac{E_1 I_1}{M+m}\right)^{1/2} t/R^2$$
$$v = \left(\frac{M}{E_1 I_1}\right)^{1/2} RV \qquad \mu = AR^2 P/E_1 I_1 \tag{24}$$

The equation of motion is as follows:

$$\frac{\partial^6 \xi}{\partial\theta^6}+(2+\mu+v^2)\frac{\partial^4 \xi}{\partial\theta^4}+(2+\mu+2v^2)\frac{\partial^2 \xi}{\partial\theta^2}+\mathrm{v}^2\xi+2\beta^{1/2}\mathrm{v}\frac{\partial^4 \xi}{\partial\tau\,\partial\theta^3}+2\beta^{1/2}\mathrm{v}\frac{\partial^2 \xi}{\partial\tau\,\partial\theta}+\frac{\partial^4 \xi}{\partial\tau^2\,\partial\theta^2}-\frac{\partial^2 \xi}{\partial\tau^2}=0 \tag{25}$$

where, "$2\beta^{\frac{1}{2}}\mathrm{v}\left(\frac{\partial^4 \xi}{\partial\tau\,\partial\theta^3}+\frac{\partial^2 \xi}{\partial\tau\,\partial\theta}\right)$" indicates the inertia created by Coriolis acceleration of the flow. The Coriolis force is directly related to $\beta^{\frac{1}{2}}$ (β is called the mass rate).

At the end, the normalized frequency for a curved pipe is obtained as follows:

$$\omega_n R^2\sqrt{(m+M)/(EI)} \tag{26}$$

In this regard, *m* and *M* are mass per unit length of pipe and fluid, respectively[14].

Finally, the boundary conditions that can be considered for a curved pipe are as follows:

For the C-C condition:

$$\xi(\theta,\tau)=0 \qquad \theta = \alpha \text{ و } \theta = 0$$
$$\eta(\theta,\tau)=0$$
$$\frac{\partial\eta(\theta,\tau)}{\partial\theta}=0 \tag{27}$$

For the C-S condition:

$$\begin{matrix} \xi(\theta,\tau)=0 \\ \eta(\theta,\tau)=0 \\ \dfrac{\partial\eta(\theta,\tau)}{\partial\theta}=0 \end{matrix} \quad \theta=0 \qquad \begin{matrix} \xi(\theta,\tau)=0 \\ \eta(\theta,\tau)=0 \\ \dfrac{\partial^3\xi(\theta,\tau)}{\partial\theta^3}=0 \end{matrix} \quad \theta=\alpha \tag{28}$$

For the S-S condition:

$$\begin{matrix} \xi(\theta,\tau)=0 \\ \eta(\theta,\tau)=0 \\ \dfrac{\partial^3\xi(\theta,\tau)}{\partial\theta^3}=0 \end{matrix} \quad \theta=0 \text{ و } \theta=\alpha \tag{29}$$

where α is the total angle of the curved pipe.

5. Definition of the problem

This paper examines a part of the fueling system of a turbofan engine connected to the pump on one side, shown in Fig.7. It is assumed that the pump has a rotational mist that produces more vibrations and its effect on the fluid causes the flow to be in turbulence and thus the outlet of the pipe. The disturbance flow of the pipe outlet continues to cause instability in the combustion.

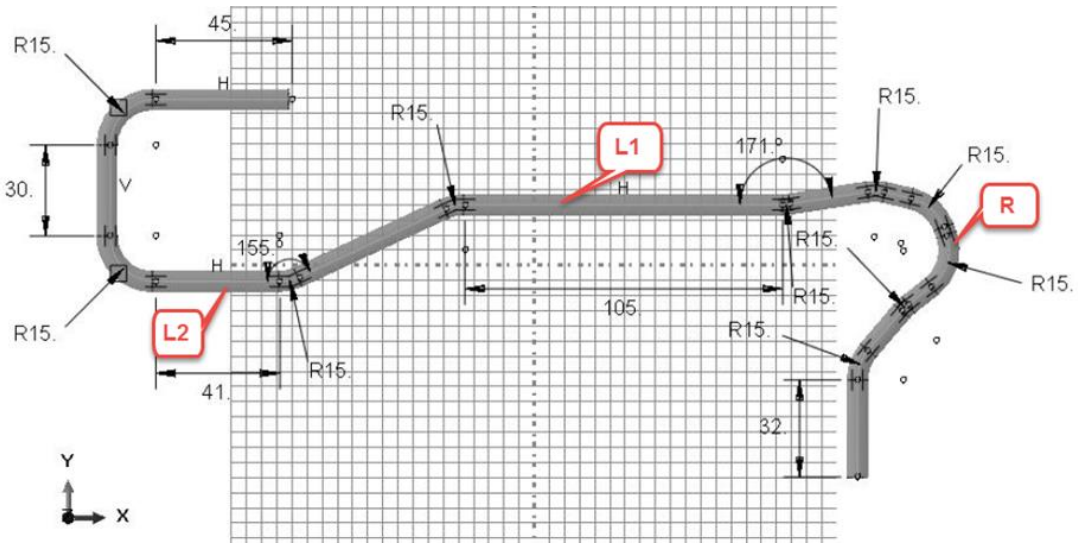

Fig. 7. the geometry of the problem

In this research, the aim is to determine the geometry and dimensions of the pipe in a specific area that alleviate the displacement amplitude and reduces the turbulence of fuel flow. In order to solve the problem, a simulation test has been carried out with Abaqus software and for the optimal dimensions of the pipe, Design Expert software has been used.

The pipe material used in this part of the fuel transfer system is usually copper, which its specifications are shown in Table 1.

Table 1. Mechanical properties of copper (pipe material of the fuel system)

Density (kg/m^3)	Modulus of elasticity(GPa)	Poisson's ratio	Thermal conductivity ($W.m^{-1}.K^{-1}$)
8900	130	0.35	391

The Jet fuel properties of a turbofan engine are given in Table 2.

Table 2. Jet fuel properties of the liquid at 40 °

Density (kg/m^3)	Thermal value (MJ/kg)	Dynamic viscosity (MPa·s)	Kinematic viscosity(mm^2/s)	Molar mass $(\frac{kg}{Kmol})$	chemical formula
800	42.80	2	4.7	167.31	$C_{12}H_{23}$

Consider the working conditions of the system in Table 3.

Table 3. System operation conditions

T(^oC)	Vin(m/s)	P(bar)
40	70	150

where T is the temperature of the fuel, Vin is the inlet flow rate, and P is the fuel pressure. Different types of fuel pumps are used for turbofan systems. One of the most widely used fuel pumps is the 831000 gear model, the specifications of which are extracted from the catalog and are presented in Table 4.

Table 4. Fuel pump operating characteristics

Speed	8400 RPM
Inlet Pressure	30 psig (207 kPag)
Boost Stage Pressure Rise	150 psig (1034 kPag)
Fuel Flow Rate	43gpm(162/min)
Weight	20.3 pounds(9.2kg)

6. Numerical Simulation and Validation

One of the issues in fluid-structure coupling problems that has a great impact on solving problems with finite element software is mesh modeling. Due to the exchange of information between fluid solution and structure solution at the domain boundary, the mesh of both geometries should be of the same size so that the nodes are placed on top of each other and there is no problem in the solution process. At this stage, in order to investigate the problem of independence from the mesh, it is necessary to examine the problem as a couple and the stress created in the pipe due to the fluid flow. The results showed that the C3D8R brick mesh with 1mm thickness is appropriate. In this study, initially, three different boundary conditions for the problem have been examined, then the C-C has been chosen as the best boundary conditions, and the effect of the different parameters on the response continues utilizing this boundary condition. The boundary conditions that will be assumed for the system are depicted in Fig. 8. *i.e.,* in addition to the two fixed ends, there are clamps 1 and 2.

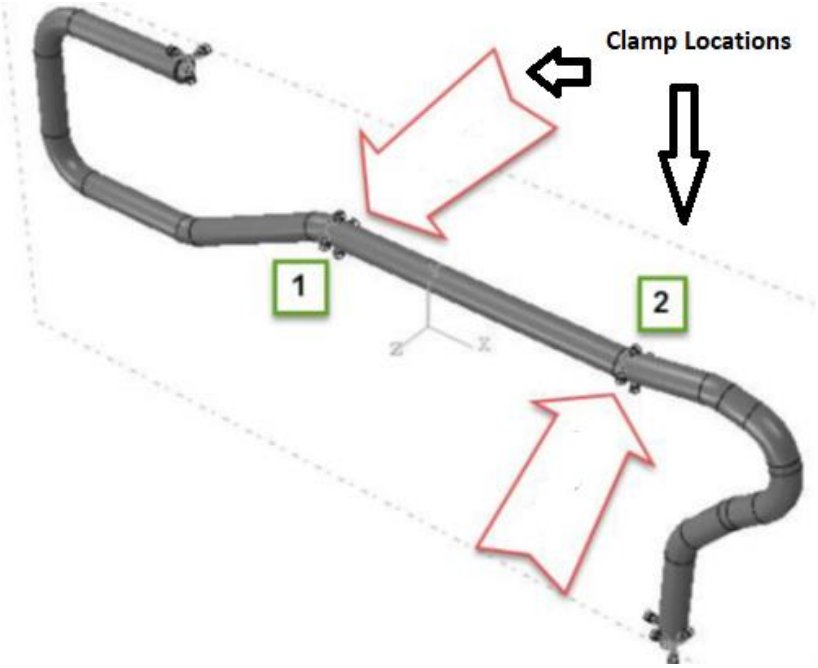

Fig. 8. Boundary conditions of the problem

For validation, the results of fluid and structure couplings solutions in the Abaqus software are compared with the results of other researchers for a straight and curved pipe with different bending angles. The pipe is selected according to the ASME B36.10M-2000 standard and the eighteen Schedule. It is a steel pipe with an outer diameter of 26.6 mm, the thickness of 3.91 mm, and the length of 2 meters have been used in simulation and equations, and the boundary conditions for this pipe are double-clamp. The fluid used in this section is water, which has a density of 1000 kg / m^3 and the inlet flow rate of 15 m /s at 20 ° C. Young's modulus for the pipe is 210GPa and the Poisson ratio 0.3 and a density of 7850 kg/m^3[13].

If we consider the first frequency of vibrations, the fundamental frequency for C-C condition can be obtained as follows [12]:

$$\omega = (\beta_1)^2 \sqrt{\frac{EI}{m+m_0}}, \ \beta_1 l = 4.730041 \tag{30}$$

Taking the high-order natural frequencies into account and neglecting the Coriolis force, the C-C condition can be written as:

$$\omega = (\beta_n)^2 \sqrt{\frac{EI}{m+m_0}}, \sqrt{1-\frac{m_0 v^2}{EI\beta_n^2}}, n = 1, 2, 3, \ldots$$
$$with\ \beta_1 l = 4.730041, \ \beta_2 l = 7.853205, \beta_3 l = 10.995608, \ \beta_4 l = 14.137165 \tag{31}$$

A comparison of the natural frequency values of Abaqus and equations (30) and (31) for the straight pipe is given in Table 5.

Table 5. Comparison of the natural frequencies obtained in Abaqus and MATLAB for the straight pipe

	Mode	1	2	3	4	5	6
Abaqus	Empty Pipe	37.51	103.15	201.53	331.73	493.06	684.64
	MATLAB Water-Filled Pipe	28.58	85.34	159.86	290.02	412.36	567.28
	Abaqus Water-Filled Pipe	29.36	85.57	157.11	288.04	415.47	560.47
	Error (%)	2.6	0.266	1.72	0.68	0.75	1.4

The normalized frequency for a curved pipe is shown in equation (26). The natural frequency for higher modes can be derived from the ω_n of uniform beam for each of the *n*th mode in the C-C boundary condition (Eq. (7)). The comparison of the results for this relationship and the Abacus solving results is presented in Table 6.

Table 6. Comparison of the normalized natural frequency obtained in Abacus and MATLAB for an

α= 90° knee			
	First mode	Second mode	Third mode
Empty Pipe	26	46	81
MATLAB Water-Filled Pipe	22	43	78.5
Abaqus Water-Filled Pipe	23.3	44.2	71.9
Error (%)	5.9	2.7	8.4

7.Results and Discussions

In the initial state, the outlet flow is shaped in such a way that its turbulent is clearly seen in Fig. 9 that shows the speed vectors at the pipe inlet and outlet. It is observed that the flow is not laminar. The purpose of this study is to reduce the turbulent of the flow in the pipe outlet.

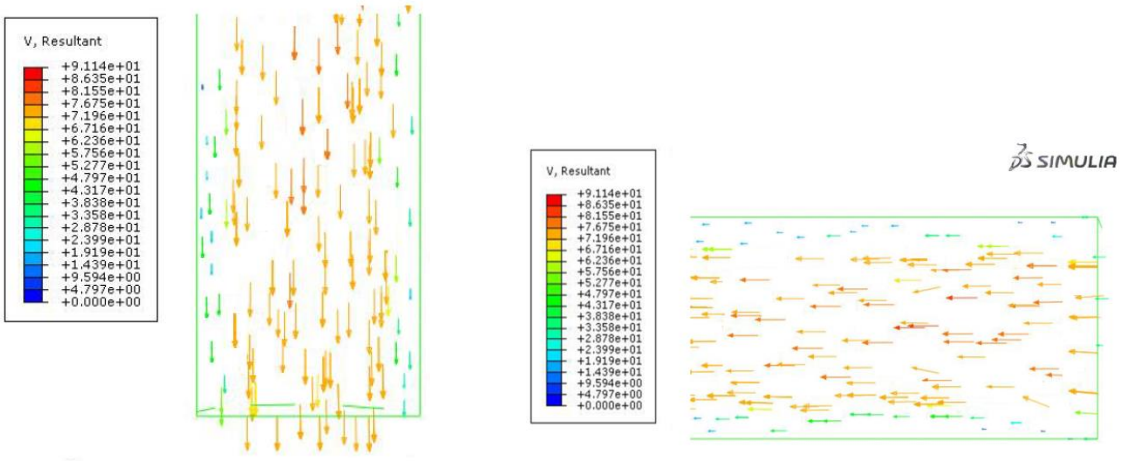

Outlet flow *Inlet flow*

Fig. 9. The velocity vectors of inlet and outlet flow

The most influential variables in the dynamic and vibrational response of the fuel flow are geometric parameters. The important geometric parameters of the fuel transfer system are pipe diameters. In this section, we study the effect of internal diameter on the vibration response of the system. Fig. 10 shows normal frequency variations by changing the inner radius of the pipe. In all of these states, the thickness of the pipe is 0.5 millimeters. It is observed that the natural frequency increased by increasing the radius.

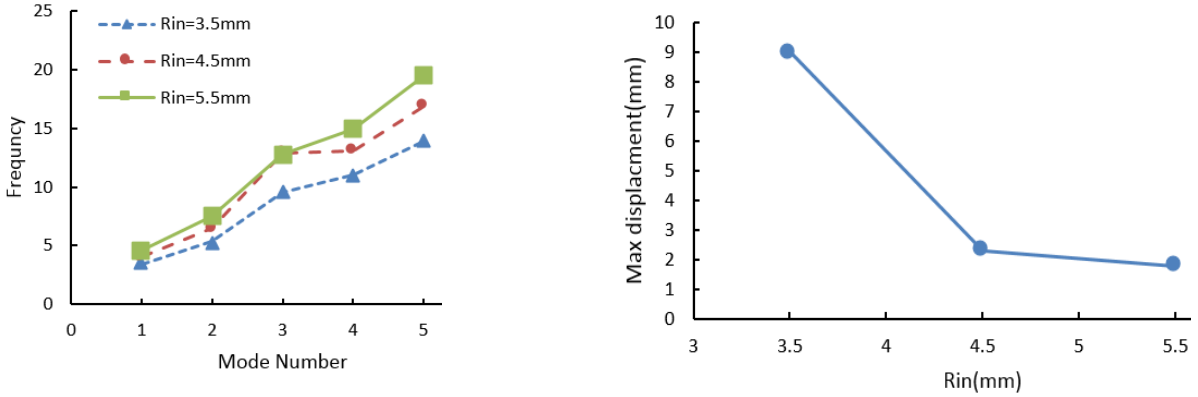

A- Variations of the frequency changes as internal radius changes in different mode number

B- Maximum displacement change as internal radius changes

Fig. 10. Frequency and maximum displacement changes with internal radius changes with Vin= 70.2 m/s.

Another geometric parameter is the thickness of the pipe; Fig.11 illustrates the variation of natural frequencies for various thicknesses of the pipe wall with an internal radius of 3.5 mm. It can be seen that as the thickness of the pipe increases, the hardness increases, so the natural frequency increases.

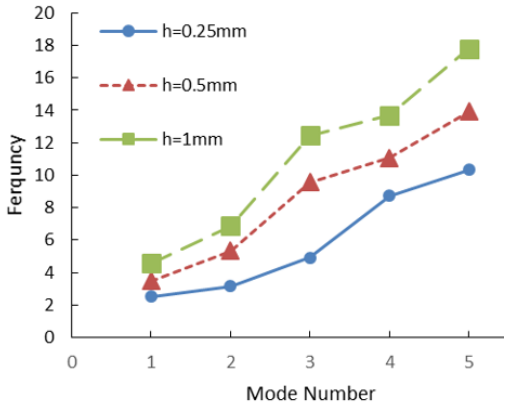

A- Variations of the frequency as the thickness of the pipe changes in different mode number

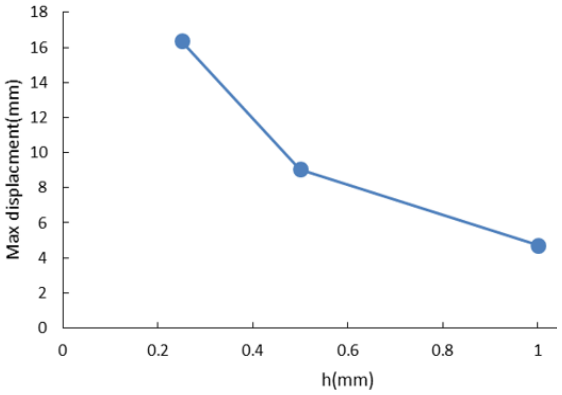

B- Maximum displacement change as the thickness of the pipe changes

Fig.11. Frequency changes and maximum displacement by changing the thickness of the pipe with Vin=70.2 m/s.

The fuel pump speed determines the flow velocity of the inlet fluid and is an important input parameter that can be changed by changing the engine speed. In Fig. 12, the effect of flow rate changes with the main frequency (*i.e.*, fuel pump speed) to the original natural frequency ratio is shown. The internal radius of the pipe is 3.5 mm and its thickness is 0.5 mm. It can be seen that with the increasing velocity of the inlet fluid, the fundamental frequency decreases. The pump speed can vary in different engine periods.

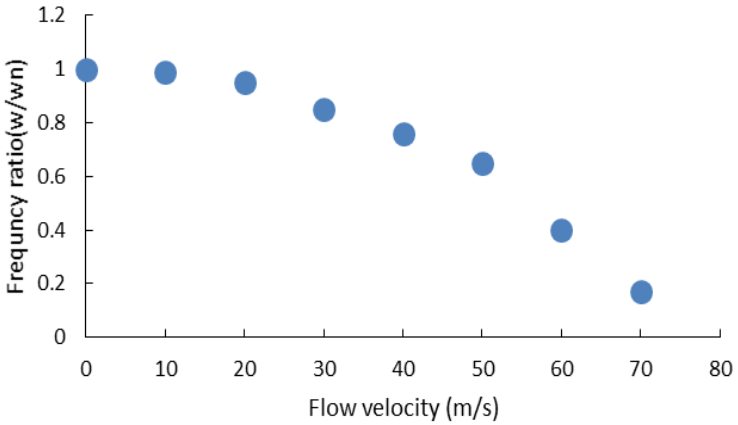

Fig. 12. Changing of the main frequency to the original natural frequency ratio at different inlet speeds of the fluid

As stated earlier, the purpose of the paper is to acquire specific dimensions for a portion of the batching system to reduce the vibration range and reduce the turbulence of the fluid in order to achieve better combustion stability for the turbofan engine. After performing several solutions by Abaqus software and investigating the effect of different geometric and functional variables on

these parameters, we need to optimize the geometric parameters of the pipe in order to have the best response range. Using the Design Expert software and NSGA II code, we obtain the relationships between the variables[15]. The software introduces the types of relationships between variables and the responses such as linear, second-order, etc., and the best relationship is achieved. In Fig.13 and Fig.14, the quality of the data presented to the software (normal of residue diagram) is shown, and it is clear that the data are of acceptable quality.

The normal residue curve is used to verify the type of relationship between the responses and the variables. If the correct data is entered, the data dispersion follows an almost straight line.

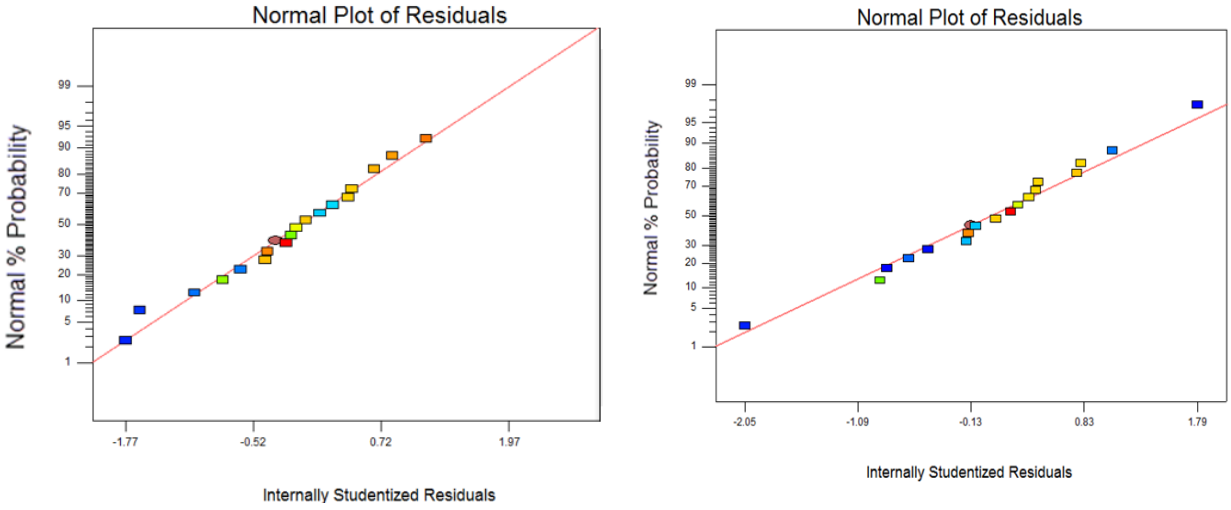

A- Normal residuals of Maximum displacement

B- Normal residuals of frequency

Fig. 13. Normal plot of residuals

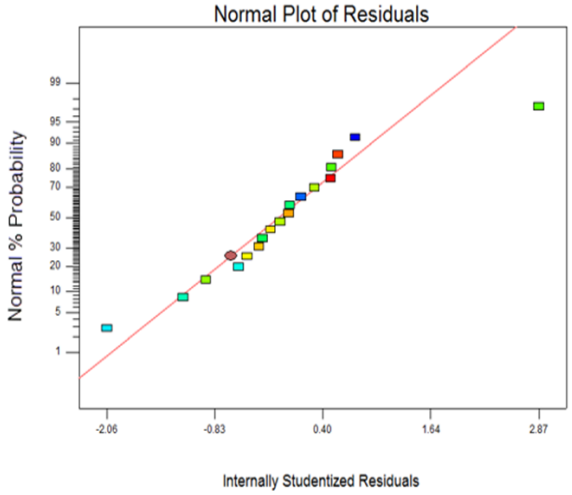

Fig. 14. The normal plot of residuals of output speed

The goal function is of maximum transverse displacement W_{max}, vibration frequency F, and outlet speed V_{out}. By introducing the solution results to the Design expert software, based on the desirability of increasing or decreasing, the goal function is determined. In this study, it is

desirable that displacement amplitude and vibration frequencies, as well as the turbulent in the outlet flow, should be reduced.

After determining these cases and by running the software, a series of optimal values of the parameters are presented with a percentage of satisfaction for the goal functions. In Table 7, four of the values provided by the software, the percentage of satisfaction with different cases are reported. In this table, the effect of changing parameters *L1*, *L2*, and *R*, as shown in Fig.7, as well as thickness of the pipe *h*; on the system responses are also considered. It should be mentioned that the goal function is at the first mode of frequency.

Table 7. Optimized reported values of Design Express

R mm	L2 mm	L1 mm	Vin m/s	P bar	R_{in} mm	h mm	Percentage of satisfaction
28	40	140	70.2	150	7	0.25	80
30	90	140	70.2	150	4	0.3	60
10	100	200	70.2	150	4.5	0.25	50
30	70	140	70.2	150	4	0.75	30

It can be seen that in the first row of Table 7, the optimal values of geometric parameters are presented with the satisfaction of 80%. The relations are obtained by the software as follows:

$$W_{max} = -10.21 - 11.8R_{in} - 0.78h + 0.76L_1 - 20.78L_2 - 0.6R + 12.2R_{in}h + 15.16R_{in}L_1 - 30.54R_{in}L_2 - 0.83hR \quad (32)$$

$$F = 7.56 + 3.21R_{in} + 0.46h + 2.54L1 + 5.74L2 - 0.16R - 0.62R_{in}h - 2.91R_{in}L_1 + 7.05R_{in}L_2 + 0.069hR + 0.38R_{in}^2 - h2 + 3.58L_1^2 + 1.31L_2^2 + 0.019R \quad (33)$$

$$V_{out} = 101.76 + 19.51R_{in} - 1.1h - 2.36L_1 + 9.11L_2 + 2.6R - 0.12R_{in}h + 7.25R_{in}L_1 + 31.68R_{in}L_2 - 0.73hR \quad (34)$$

After deriving the relations of the objective function with different variables, according to the type of these relations, the software provides a series of surfaces as functions of maximum displacement and outlet speed of the fluid. The results of these optimum values of the geometric parameters are shown in Figures 15 to 17.

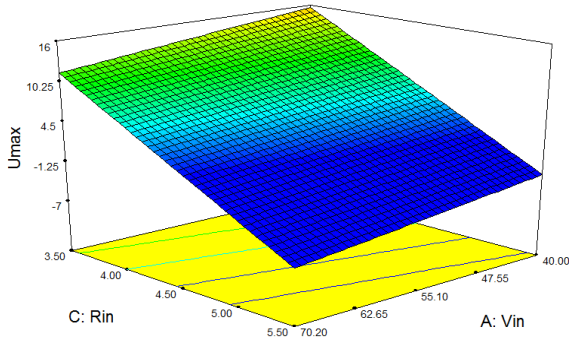

Fig.15. Variations of W_{max} w.r.t. the inner diameter and inlet speed of the fluid variables.

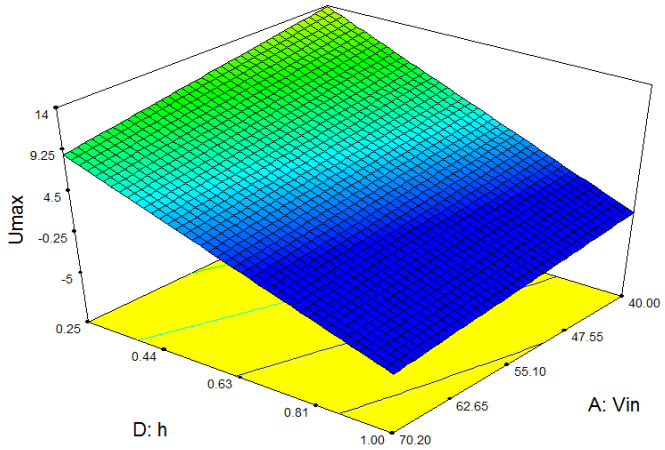

Fig.16. Variations of Wmax w.r.t. the thickness of pipe and inlet speed of the fluid variables

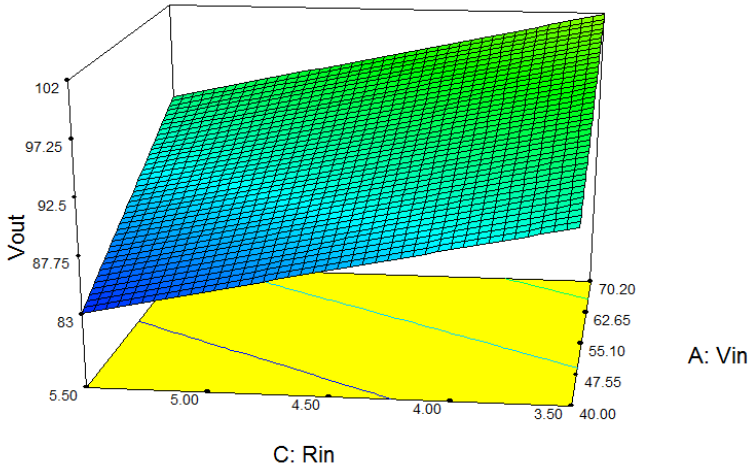

Fig.17. Variations of V_{out} w.r.t. the inner radius of pipe and inlet speed of the fluid variables

Finally, the diagrams of the output changes in optimal conditions using the NSGA II code are obtained, as presented in Figures 18 and 19. It can be seen that Figures 18 and 19 show the relationships between outlet velocity of the fuel system and the vibration frequency as well as maximum transverse displacement of the system in optimal conditions, respectively. In both diagrams, V_{out} is in m/s, Frequency in Hz, and W_{max} in mm.

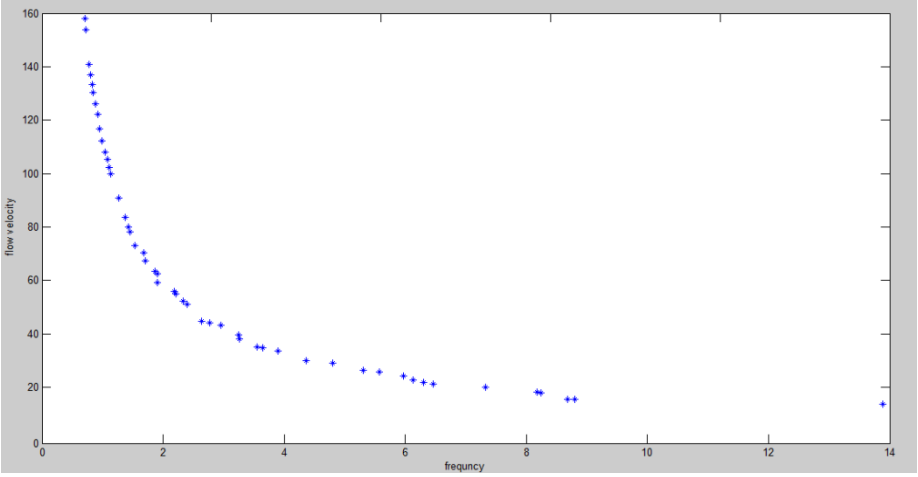

Fig.18. The optimum values of V_{out} w.r.t. the vibration frequency in optimal conditions

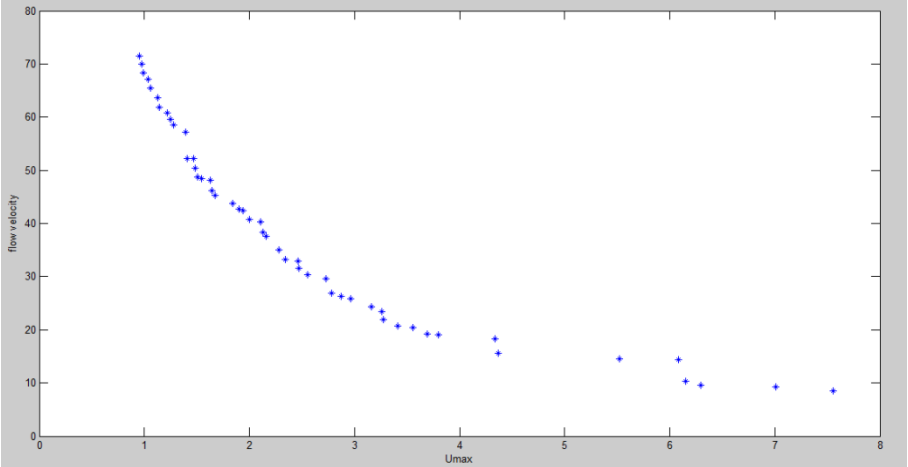

Fig.19. The optimum values of V_{out} w.r.t. the Wmax in optimal conditions

8. Conclusion

In this paper, the vibrations induced by fluid flow in part of the fuel system and caused by an unbalanced fuel pump ultimately resulting in an improper fuel spill and combustion instability were studied. The effects of parameters, such as the inside diameter of the pipe, the pipe thickness, the flow rate of the inlet, etc., were studied on the dynamic response of maximum transverse displacement and frequency. The results demonstrates that the vibration frequency of this part of the fuel transmission system is very low and the natural frequency varies-between 2.5 and 18 Hz. It is far from the frequency of the pump (about 140 Hz) and the possibility of resonance is very slight. However, the maximum transverse displacement (range) is relatively significant (up to about 16 mm). By increasing the flow rate in the pipe, the natural frequency has also decreased. The important geometric parameters of the fuel transfer system are the

straight length, curved radius, inner diameter as well as thickness of the pipe. In this regard, the effect of internal diameter and thickness of the pipe has been studied. The results illustrates that the natural frequency increases as both the internal radius and thickness of the pipe are increasing. After processing the data, the optimal values are obtained in the acceptable range for output parameters and problem variables. The pipe thickness is 0.25 mm, the internal radius is 7 mm at a pressure of 150 bar, and the maximum speed is 70.2 m / s for the pipe section. The dimensions of the track are L1 =140, L2 =40, and R =28 as the optimal mode with the satisfactory percentage of 80%. Other results can also be related to the reduction of turbulence in the outlet stream, which can significantly contribute to better combustion.

References

[1] H.J.-P. Morand, R. Ohayon, Fluid structure interaction-Applied numerical methods, Wiley, 1995.
[2] E.H. Dowell, K.C. Hall, Modeling of fluid-structure interaction, Annual review of fluid mechanics, 33 (2001) 445-490.
[3] C. Michler, S.J. Hulshoff, E.H. Van Brummelen, R. De Borst, A monolithic approach to fluid–structure interaction, Computers & fluids, 33 (2004) 839-848.
[4] S. Chakrabarti, Hybrid numerical method for wave–multibody interaction, WIT Transactions on State-of-the-art in Science and Engineering, 18 (2005).
[5] G. Hou, J. Wang, A. Layton, Numerical methods for fluid-structure interaction—a review, Communications in Computational Physics, 12 (2012) 337-377.
[6] B.M. Tashakori, M.R. Elhami, A.R. Rabiee, Numerical Analysis of Fluid Structure Interaction Phenomenon on a Turbine Blade, (2016).
[7] I.R. Dubyk, I.V. Orynyak, Fluid-structure interaction in free vibration analysis of pipelines, Вісник Тернопільського національного технічного університету, 81 (2016) 49-58.
[8] S. Moore, A review of noise and vibration in fluid-filled pipe systems, Proceedings of the Acoustics, Brisbane, Australia, (2016) 9-11.
[9] K.S. Fong, A.Y.M. Yassin, Fluid-structure interaction (FSI) of damped oil conveying pipeline system by finite element method, in: MATEC Web of Conferences, EDP Sciences, 2017, pp. 01005.
[10] S. Olsson, J. Kesti, Fluid structure interaction analysis on the aerodynamic performance of underbody panels, in, 2014.
[11] R.S. Raja, Coupled fluid structure interaction analysis on a cylinder exposed to ocean wave loading, (2012).
[12] H. Yi-Min, L. Yong-Shou, L. Bao-Hui, L. Yan-Jiang, Y. Zhu-Feng, Natural frequency analysis of fluid conveying pipeline with different boundary conditions, Nuclear Engineering and Design, 240 (2010) 461-467.
[13] S.s. Chen, Vibration and stability of a uniformly curved tube conveying fluid, The Journal of the Acoustical Society of America, 51 (1972) 223-232.
[14] M.R. Ghazavi, H. Molki, Nonlinear vibration and stability analysis of the curved microtube conveying fluid as a model of the micro coriolis flowmeters based on strain gradient theory, Applied Mathematical Modelling, 45 (2017) 1020-1030.
[15] A. Kharestani, Vibration analysis and study of FSI in engine fuel system for combustion stability in a turbofan, in: , Mech. Eng. Dept., IHU (in Persian), 2018.